Journal of Atmospheric and Solar-Terrestrial Physics 167 (2018) 177–183

Contents lists available at ScienceDirect

Journal of Atmospheric and Solar-Terrestrial Physics

journal homepage: www.elsevier.com/locate/jastp

Properties of frequency distribution of Pc5-range pulsations observed with the Ekaterinburg decameter radar in the nightside ionosphere

Maksim A. Chelpanov *, Olga V. Mager, Pavel N. Mager, Dmitri Yu. Klimushkin, Oleg I. Berngardt

Institute of Solar-Terrestrial Physics, 664033, Irkutsk, p/o box 291, Lermontov st., 126a, Russia

ARTICLE INFO

Keywords:
ULF waves
High-frequency radar
Magnetosphere

ABSTRACT

A statistical study of waves in the magnetosphere registered with the midlatitude coherent decameter radar located near Ekaterinburg (EKB), Russia is presented. The radar monitors ionospheric flow velocities whose small-scale variations are evoked by magnetosphere ultra low frequency (ULF) waves of Pc5-range. Data from 16 events observed during 7 months in 2014 and 2015 underwent wavelet analysis. Frequencies of the oscillating components were compared with Alfvén eigenfrequencies, which were inferred from THEMIS and Van Allen spacecraft data. The comparison showed that only a minor part of the oscillations registered with the radar in the nightside ionosphere could be attributed to the Alfvén mode. A majority of the waves have lower frequencies, which do not show dependence on Alfvén eigenfrequency of a field line.

1. Introduction

Radars are a useful tool for studying the ultra low frequency (ULF) waves in the terrestrial magnetosphere (e.g., Yeoman et al., 2016). At present, the waves are widely studied with the Super Dual Auroral Radar Network (SuperDARN) (e.g., Bland et al., 2014). For example, Norouzi-Sedeh et al. (2015) used SuperDARN data for studying the occurrence and frequencies of midlatitude ULF waves in the Pc5 range ($\sim 1-7$ mHz), and Bland and McDonald (2016) conducted statistical examination of the Pc5 waves in the southern polar cap. Several recent ULF wave case studies involving SuperDARN are presented in (Yeoman et al., 2010, 2012; Sakaguchi et al., 2012; Teramoto et al., 2014).

Already early radar observations showed that the Pc5 ULF waves can be divided into the waves with small and high values of the azimuthal wave number, m (e.g., Walker et al., 1982; Fenrich et al., 1995). The former represent oscillations generated by external processes such as Kelvin-Helmholtz instability or buffeting of the magnetosphere by the solar wind; alternatively, they can directly penetrate to the magnetosphere from the solar wind (for recent overview, see (Nakariakov et al., 2016)). On the contrary, the high-m waves must be internally generated, probably particle-driven oscillations (e.g., Yeoman et al., 2000; Baddeley et al., 2004; James et al., 2016).

The high-m ULF waves are observed also in situ with satellites (e.g., Liu et al., 2013; Dai et al., 2015; Chi and Le, 2015; Moiseev et al., 2016). The storm time compressional Pc5 pulsations represent a sub-class of the high-m waves (Anderson, 1993). They have considerable compressional component of the magnetic field perturbation oscillating in antiphase with the plasma pressure. Their frequencies are sufficiently lower than the characteristic eigenfrequencies of the Alfvén modes. A probable physical interpretation of those wave is the drift compressional mode, the most common compressional mode in finite-β inhomogeneous plasma (Crabtree and Chen, 2004; Crabtree et al., 2003; Klimushkin and Mager, 2011; Mager et al., 2013).

Recent radar observations confirm that a part of the high-m Pc5 waves can be interpreted as the drift compressional modes (Mager et al., 2015; Chelpanov et al., 2016). However, the majority of the radar studies still identify the high-m Pc5 waves with the Alfvén modes (e.g., James et al., 2013, 2016). The aim of this paper is to perform a statistical analysis to determine a relative number of the Alfvén and drift compressional modes in the nightside magnetosphere with the help of a recently launched Ekaterinburg (EKB) midlatitude decameter radar.

2. Instrumentation

The Ekaterinburg midlatitude decameter radar was designed similar to Super Dual Auroral Network (SuperDARN) radars. It radiates series of pulses that are scattered in the ionosphere and measures Doppler line-of-sight (l-o-s) velocity of ionospheric irregularities by characteristics of a

* Corresponding author.
E-mail addresses: max_chel@iszf.irk.ru (M.A. Chelpanov), o.mager@iszf.irk.ru (O.V. Mager), p.mager@iszf.irk.ru (P.N. Mager), klimush@iszf.irk.ru (D.Yu. Klimushkin), berng@iszf.irk.ru (O.I. Berngardt).

https://doi.org/10.1016/j.jastp.2017.12.002
Received 13 April 2017; Received in revised form 2 November 2017; Accepted 2 December 2017
Available online 9 December 2017
1364-6826/

return signal. The radar monitors a 50° field of view by sequential scanning of 16 observation sectors, or beams. Radar field of view length is about 3100 km in radial direction, it is divided into 75 fixed range gates, 45 km each. The initial gate begins at 180 km from the radar sight. The field of view of the radar is shown in Fig. 1.

Given that in the normal mode the radar sounds all the 16 beams consecutively with a dwell time of 6 s for each beam, a time resolution of 96 s is provided. The EKB radar implements sounding in additional special operation mode for the three adjacent beams whose directions are most close to magnetic meridian (beams 0, 1 and 2) (Mager et al., 2015). With the same 6 s integration time it provides an 18 s time resolution for each of the three beams. This mode enables observation of ionosphere flow velocity fluctuations along beam directions with periods of 36 s and above. Such fast velocity variations of small-scale irregularities are caused by the $\vec{E} \times \vec{B}$ drift evoked by magnetospheric ULF waves (e.g., Wright and Yeoman, 1999; Ponomarenko et al., 2003, 2005; Yeoman et al., 2012; Bland et al., 2014). As one of the high resolution beams is directed toward the magnetic pole, and two other ones are close to magnetic meridian direction, the measured velocity fluctuations represent the ionospheric flow meridional component, which is related to the azimuthal component of the wave electric field. This component in turn corresponds to the radial component of a magnetic field disturbance. Hence, we should note that the toroidally polarized waves cannot be observed with the poleward beams.

3. Data analysis

The events of wave observations studied in this paper occurred between 4 September 2014 and 14 March 2015. The oscillations were observed in the nightside ionosphere within time period 1900-0330 UT, which approximately corresponds to 2230-0700 MLT. All the waves were registered within gates 12–32, or L shells 3.63–6.61 (according to the International Geomagnetic Reference Field (IGRF)). We selected 16 events in order to fit the requirement of satellite data presence for the longitudinal sector and L shell of the observations (see below). Fig. 2 shows spatio-temporal location of the investigated ionospheric scatter (solid line areas) and position of ground scatter during these experiments (dashed line areas). Ground scatter has a very specific dependence on the range and time for the EKB radar investigated in details in (Berngardt et al., 2015). As one can see, the ionospheric scatter investigated in the discussed experiments can be easily differed from ground scatter that is observed during these experiments at larger distances. As an example, the upper panel of Fig. 3 presents more detailed flow velocity variations observed at beam 1 on 25 December 2014. Positive (negative) values indicate velocities directed toward (away from) the radar. Panel b shows a plot of periodic velocity variations for one of the range gates.

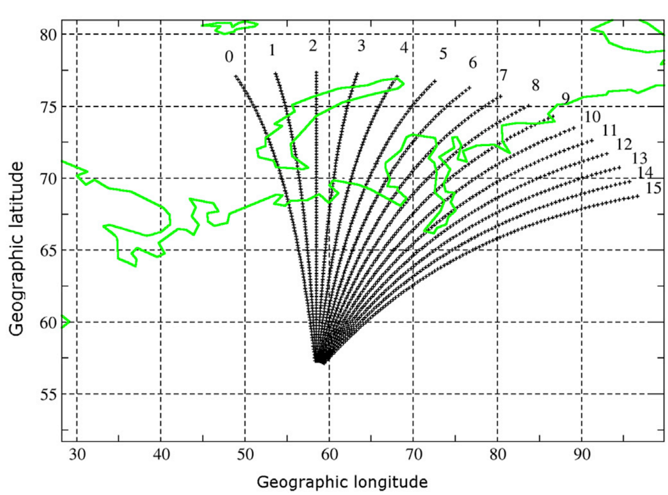

Fig. 1. Full view of the EKB radar in geographic coordinates. Numbers 0 to 15 indicate beams.

The time series for each of the events studied underwent interpolation with a grid spacing of 20 s in order to equalize the sampling intervals, after that the high-pass filter with a 600 s cutoff period was applied. Then discrete Morlet wavelet transform was used (Grossman and Morlet, 1984; Foster, 1996):

$$W(\omega,\tau) = \sqrt{\omega}\sum_{j=1}^{N} x(t_j)\, e^{i\omega(\tau-t_j)-(\tau-t_j)^2/2T^2}, \tag{1}$$

where ω is the frequency, τ is the time shift, $x(t_j)$ is a discrete data set of N times t_j, where $j = 1, 2...N$, $T = 2\pi/\omega$ is the period.

Poleward adjacent high frequency beams is a convenient facility that, among other parameters, lets us measure azimuthal wave number m. We can use Morlet wavelet transform to calculate phase difference between the signals obtained at two beams:

$$W_{12}(\omega,\tau) = W_1(\omega,\tau)W_2^*(\omega,\tau), \tag{2}$$

where W_1 and W_2^* are wavelet transform and complex conjugate wavelet transform for two beams data, respectively. The phase of $W_{12}(\omega,\tau)$ represents the phase difference $\Delta\phi$ of the two signals. Azimuthal wave number (Olson and Rostoker, 1978)

$$m = -\frac{\Delta\phi}{\Delta\lambda}, \tag{3}$$

where $\Delta\lambda$ is longitude separation between two beams at given L shell. This method, however, features a systematic error that can reach 25%: due to the fact that exact altitude of the reflection point in the ionosphere is unknown, it's coordinates along beam direction could be defined incorrectly with an error of up to 200 km. This results in an error in longitude separation calculation of about 10 km.

To reveal common oscillation spectra we used the wavelet amplitude function

$$F_{12}(\omega,\tau) = F_1(\omega,\tau)F_2(\omega,\tau), \tag{4}$$

where $F_1(\omega,\tau)$ and $F_2(\omega,\tau)$ are amplitude functions for adjacent beams:

$$F(\omega,\tau) = \frac{2|W|}{\sqrt{\omega}n(\omega,\tau)}, \tag{5}$$

here

$$n(\omega,\tau) = \sum_{j=1}^{N} e^{-(\tau-t_j)^2/2T^2}. \tag{6}$$

The function $F_{12}(\omega,\tau)$ describes the oscillation components that form the resulting signal. A plot of such function for the 25 December event for one of the gates is given in Fig. 3c. It shows explicitly a distinct oscillating harmonic with the frequency of about 3.8 mHz. The spectra for a few more events also exhibit one main oscillating harmonic, while the other feature multi-harmonic structure.

In order to study characteristics of the oscillation observation events we considered such $F_{12}(\omega,\tau)$ plots for pairs of high resolution beams. This gives an advantage of better noise elimination over using data from a single beam. We used data sets from the range gates where the oscillations were clearly seen and the data coverage was sufficient. Although some of the events were being registered for more than 3 h, each of the constituent distinct oscillating harmonics did not last longer than several periods. As frequency resolution of wavelet transform is limited to 1–1.5 mHz in our research, and variations in frequencies of the harmonics during their observations were moderate, we estimated a single value of frequency for each component. They were determined at the maxima of oscillation intensities. Again, given the limitation of Morlet